

Oxidative competition between aliphatic and aromatic C–H bonds in the N₂O–Fe–ZSM-5 system

A. Costine*, T. O’Sullivan, B.K. Hodnett

Materials and Surface Science Institute, University of Limerick, Castletroy, Limerick, Ireland

Available online 16 December 2004

Abstract

The peculiar electrophilic behaviour of active oxygen formed over Fe-ZSM-5 zeolites upon nitrous oxide decomposition has been investigated in toluene oxidation. Fe-ZSM-5 catalysts have been produced by hydrothermal and post-synthetic techniques, with particular attention given to preparation by chemical vapour deposition of anhydrous FeCl₃ into H-ZSM-5. Higher yields of hydroxylated product are possible over Fe-zeolites prepared by hydrothermal synthesis, with *para*-cresol being the predominant oxygenate formed, though the formation of tars and polycondensed aromatic hydrocarbons retards catalytic activity over time. Oxidation of *para*-xylene, isopropylbenzene, benzaldehyde, chlorobenzene and phenol demonstrate that the oxidative competition between aliphatic and aromatic C–H bonds is influenced considerably by the steric and electronic nature of the substituent groups.

© 2004 Elsevier B.V. All rights reserved.

Keywords: Fe-ZSM-5; Nitrous oxide; Selective oxidation; Aromatic substrates

1. Introduction

The activation of oxygen on the catalyst surface is an essential stage for the heterogeneous reactions of selective oxidation [1,2]. However, the central problem associated with selective oxidation reactions that form the basis of commercial production units is the tendency for the active oxygen species involved to further oxidize the desired oxidation product. This process is sometimes referred to as over-oxidation and can be minimized, but not eliminated, by suitable choice of the catalyst and reactor engineering, but is ultimately limited by the chemical nature of the oxidizing species generated on these catalysts.

In general, oxygen species in conventional selective oxidation reactions activate a hydrocarbon molecule by rupture of the weakest C–H bond in a particular reactant. Studies in kinetic isotope effect (KIE) demonstrate that for those substrates possessing more than one type of C–H bond in their structure, the weakest bond is preferentially activated. For *n*-butane oxidation [3] and propane ammoxidation [4] this is the methylene (–CH₂–) bond, whereas the

slow step in propene oxidation to acrolein [5,6] involves rupture of the weaker methyl (–CH₃) bonds. Over-oxidation is thought to proceed by attack of the active oxygen species on the weakest bond in the selective oxidation product via a mechanism very similar to the way in which the original hydrocarbon was activated. Results by Sokolovskii [7] are particularly illustrative of this, where an impressive correlation between the rate of total oxidation of *n*-alkanes on cuprous oxide and the bond dissociation enthalpy of the weakest C–H bond was found; the weaker the C–H bond strength in the alkane, the more readily it is oxidized.

Lee and Grobowski [8] have demonstrated a relationship between the reactivity of O[–] radical towards saturated hydrocarbons and the C–H bond dissociation energy of the hydrocarbon; as the C–H bond strength decreases in the hydrocarbon chain, the reactivity towards O[–] increases. Monnier [9] has presented interesting catalytic data for the epoxidation of a variety of olefins over promoted Ag/Al₂O₃ catalysts using molecular oxygen as the oxidant. A striking feature of this work is that the presence of an allylic C–H bond in the starting substrate eliminates the possibility of achieving a high selectivity in epoxidation. This is because the reaction is directed towards cleavage of the allylic C–H bond rather than the addition of oxygen. Selectivity is the

* Corresponding author.

E-mail address: allan.costine@ul.ie (A. Costine).

major criterion whereby these catalysts are judged. According to the above argument it is associated with the ability of the oxygen species in these reactions to discriminate between the weakest C–H bond in the reactant and product and high selectivity is only achieved in circumstances where the product is structurally more stable than the reactant (by ~ 30 kJ/mol [10]). The chemistry involved in these reactions is strictly that of the attack of the weakest bond in the reactant or product and therein lays the ultimate limitation of this type of chemistry.

Of special interest is the highly reactive surface oxygen species formed upon N_2O decomposition over iron complexes stabilized within the ZSM-5 matrix [11–13]. This oxygen (called α -oxygen by the authors) exhibits a high reactivity typical of enzyme monooxygenases, and mimics its unique ability to perform selective oxidation of hydrocarbons. At room temperature, α -oxygen reacts with CH_4 and CO and offers a promising alternative to the multi-step cumene process for the production of phenol. Interestingly, the α -oxygen species gives a very unusual reactivity trend when exposed to a hydrocarbon with more than one type of C–H bond. In a study of the oxidation of alkylaromatics with α -oxygen under ambient conditions the reactivity of the aromatic nucleus was found to be higher than that of the aliphatic substituents [13]. An oxygen species with a preferential reactivity towards the stronger C–H bonds in a substrate or capable of discriminating in favour of the stronger bonds of a hydrocarbon, in the presence of a product with less stable bonds would extend the range of reactions susceptible to selective oxidation.

The selective oxidation of aromatic hydrocarbons is of particular interest, because it provides a way to mono- or diphenols that are valuable products or intermediates for the synthesis of drugs, polymers, pesticides, etc., most of which are currently manufactured via multi-step processes. It has been demonstrated [14–17] that nitrous oxide may be used as a mild oxidizing agent in the transformation of benzene into monophenol or halogenated benzenes into corresponding halogenated phenols. Table 1 displays the percentage yields and product distributions that resulted from the oxidation of toluene in various catalytic environments. This literature review illustrates the preference of conventional oxygen species for the weaker bonds in a substrate, with the formation of benzylic products always exceeding oxidation of the aromatic nucleus. Despite differences in the type of oxidant employed and the reaction temperatures, the chemistry of the active oxygen species in each case is attack at the weaker benzylic C–H bonds. Table 1 also introduces some results obtained through this work, where the selective oxidation of toluene using $\text{N}_2\text{O}/\text{Fe-ZSM-5}$ catalysts prepared by chemical vapour deposition and hydrothermal synthesis, yields predominantly oxygenated products from ring-oxidation.

While Brønsted acid sites have been indicated as necessary for these hydroxylation reactions [16,28], the original hypothesis of Panov et al. [13], attributing catalytic activity

to iron sites in the extra-framework position, the so-called α -sites, is now widely accepted [29–33]. Panov and coworkers have ascribed the catalytic performance of Fe-ZSM-5 to the presence of binuclear iron species, located within the zeolite micropores and formed by the extraction of iron from the zeolite matrix during the activation treatment. It is known that zeolites containing α -sites can be prepared by iron addition at the synthesis stage or by its post-synthetic introduction [34], though comparatively lower yields of phenol in benzene oxidation have been reported for the latter [35].

Binuclear Fe oxo-hydroxo species located at the Brønsted sites have been proposed to be the active phase in Fe-ZSM-5 prepared by chemical vapour deposition (CVD) of anhydrous FeCl_3 [36–38]. Along with aqueous ion-exchange [39] and solid state ion-exchange [40,41], CVD of volatile FeCl_3 belongs to the so-called post-synthesis loading techniques. The exact nature and reactivity of the Fe-active phase is still debated in the literature. The central problem hindering identification of a structure/reactivity relationship for the active Fe phase is the presence of Fe spectator species in catalysts prepared by both FeCl_3 CVD and hydrothermal synthesis [38,42,43]. The agglomeration of Fe-binuclear complexes, especially during the calcination procedure, has been reported [42], which results in the formation of catalytically inactive goethite and hematite [13,36,44]. However, it has been shown recently [42] that the agglomeration of Fe-species in Fe-ZSM-5 (CVD) can be suppressed considerably, though not entirely eliminated, by employment of a mild calcination treatment.

This communication describes the catalytic oxidation of toluene, a reactant possessing both benzylic and aromatic C–H bonds, with Fe-ZSM-5 catalysts prepared by post-synthetic techniques and hydrothermal synthesis. To investigate the oxidative competition between aliphatic and aromatic C–H bonds, as well as the influence of electronic and steric factors affecting these transformations, a variety of organic substrates were tested.

2. Experimental

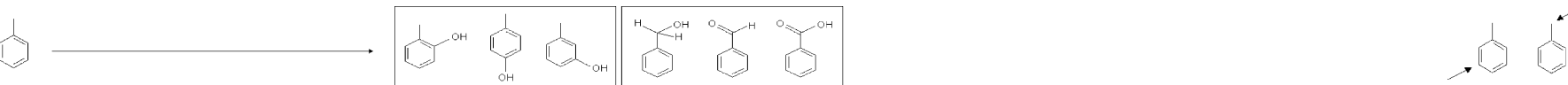
2.1. Catalyst preparation

Fe-ZSM-5 catalysts were prepared by (A) liquid phase ion-exchange, (B) solid state ion-exchange, (C) chemical vapour deposition and (D) hydrothermal synthesis.

(A) The hydronium form of ZSM-5 (0.003 wt.% Fe) was provided by PQ Corporation (Si/Al = 30). Fe-ZSM-5 was prepared by liquid phase ion-exchange with a dilute solution of $\text{Fe}(\text{SO}_4)$ (Baker) at 50°C under N_2 atmosphere. The exchange was carried out in a laboratory autoclave with continuous stirring. After 20 h the ion-exchanged product was filtered, washed with deionized water and dried at 100°C in vacuum. For all catalyst samples special attention was given to

Table 1

Summary of reactivity of oxygen species towards ring or benzylic C–H bonds in toluene



Reaction environment					Product Yield (%)								Attack
Ref.	Catalyst system	Type	Oxidant	Temperature (°C)	ortho-Cresol	para-Cresol	meta-Cresol	Benzyl-alcohol	Benz-aldehyde	Benzoic acid	Others	Ring:methyl	
[18]	Co(OAc) ₂ /NaBr in water-ScCO ₂	Homogeneous	O ₂	120	0	0	0	1.8	2.3	87	0	0:100	
[19]	5 wt.% V ₂ O ₅ /2 wt.% TeO ₂ /TiO ₂	Supported	O ₂	350	0	0	0	0	1	59.4	17.9	0:100	
[20]	Mn(TDCPP)Cl	Homogeneous	H ₂ O ₂	25	0	0	0	2.2	0	15.2	12.7	4:96	
[21]	V-AlPO-31	Mesoporous	Air	400	0	0	0	0	15.8	2	5	0:100	
[22]	Mn-layered double hydroxide	Hydrotalcite	TBHP	80	0	0	0	0.2	3.4	10.7	0	0:100	
[23]	Cr-ZSM-5 (hydrothermal)	Zeolite	TBHP	80	<0.1	<0.1	0	1	4.3	4.7	8.3	1:99	
[24]	V-ZSM-48	Zeolite	TBHP	80	0	0	0	1.7	2.7	3.2	0.1	0:100	
[23]	V-ZSM-5 (hydrothermal)	Zeolite	TBHP	80	0	0.7	0	1.3	3.6	2	0.8	9:91	
[25]	FePc-NaY zeolite	Zeolite	H ₂ O ₂	80	Total cresol 1.4			4.4	2.4	0	0	17:83	
[26]	V on titania/silica	Supported	O ₂	280	0	0	0	0	BzAl and BzAc 6.6		1.7	0:100	
[19]	5 wt.% V ₂ O ₅ /TiO ₂	Supported	O ₂	350	0	0	0	0	1.8	2.9	2.5	0:100	
[19]	5 wt.% V ₂ O ₅ /Al ₂ O ₃	Supported	O ₂	350	0	0	0	0	2.7	1.8	5	0:100	
[27]	Nb-MCM-41	Mesoporous	H ₂ O ₂	70	0	0	0	3	<0.1	<0.1	0	0:100	
[23]	Cr-ZSM5 (impregnation)	Zeolite	TBHP	80	<0.1	0.1	0	0.3	1.6	1.2	0	3:97	
[13]	0.56% Fe-ZSM-5/(HT) ^a	Zeolite	N ₂ O	25	NA	NA	NA	NA	NA	NA	NA	2.6:1	
This work	0.13% Fe-ZSM-5/(CVD) ^a	Zeolite	N ₂ O	350	0.3	1.6	0.5	0	0	0	4.1	100:0	
This work	0.7% Fe-ZSM-5/(CVD) ^a	Zeolite	N ₂ O	350	0.7	2.7	0.8	0	0	0	18	100:0	
This work	0.4% Fe-ZSM-5/(HT) ^a	Zeolite	N ₂ O	350	0.6	4.6	0.9	0	0	0	17	100:0	

NA: not available.

^a Denotes results obtained in this work using 0.5 g Fe-ZSM-5 prepared by chemical vapour deposition (CVD) and hydrothermal synthesis (HT), calcined at 900 °C, 15% N₂O, 2% toluene, balance N₂, temperature 350 °C, total flow 60 ml/min, time on stream 30 min.

the calcination procedure. Activation of the samples was performed in a plug flow reactor using a N_2 flow of 100 ml/min, where the sample was heated with a low temperature ramp ($1^\circ\text{C}/\text{min}$) to 250°C . At this temperature, 50 ml/min of air was added to the N_2 flow while, under the same temperature ramp, heating was continued to 900°C . After 2 h at 900°C the temperature was decreased to 30°C and the resulting samples were stored in air.

- (B) Preparation of Fe-ZSM-5 by solid state ion-exchange involved intense grinding of dried H-ZSM-5 zeolite with anhydrous FeCl_3 (>99.99%, Aldrich) in a mortar for 1 h (H-ZSM-5:iron chloride 3:1). The mixture was then transferred into a beaker and excess FeCl_3 was dissolved in water. After 5–10 min the supernatant solution was poured off and the dissolution procedure was repeated. Typically, catalysts were washed with 500 ml water in three washing cycles. The wet powder was then dried at 100°C in vacuum and calcined as previously outlined.
- (C) Preparation by chemical vapour deposition (CVD) involved sublimation of volatile FeCl_3 into the cavities of H-ZSM-5 as described by Chen and Sachtler [36]. The CVD exchange was performed in a U-shaped quartz reactor, with a porous frit providing separation of the H-ZSM-5 support and the FeCl_3 precursor. In order to remove moisture, 1.5 g of the H-ZSM-5 (sieve fraction between 100 and $250\ \mu\text{m}$) was loaded onto one leg and flushed overnight under N_2 (50 ml/min) at 300°C . After the temperature was lowered to 30°C under the same N_2 flow, the reactor was isolated and moved to a N_2 glove bag, where 0.35–0.7 g of anhydrous FeCl_3 was added to the second leg. The reactor was reconnected to the N_2 flow and sublimation exchange was performed at 330°C for 5–30 min. Following sublimation, the sample was washed in deionized water and dried overnight at 100°C in vacuum. The Fe-ZSM-5 samples were calcined at 900°C as already described.
- (D) Two types of iron containing zeolites, an aluminium-containing species (ZSM-5) and an aluminium-free species (silicalite) were synthesized. The synthesis mixture for both the silicalite and ZSM-5 contained sodium metasilicate nonahydrate (minimum 98%, Sigma), iron (III) sulphate (analytical grade, Reidel-de Haën) and sulphuric acid (puriss. 95–97%, Fluka). Aluminium nitrate (puriss. $\geq 98.0\%$, Fluka) was used as the aluminium source for the ZSM-5. Tetrapropylammonium bromide (TPABr, purum $\geq 98\%$, Fluka) provided the organic template for both zeolites. The synthesis gel for ZSM-5 had nominal molar ratios for $\text{H}_2\text{O}:\text{Si}:\text{TPABr}:\text{Al}:\text{Fe} = 4800:100:7.1:2:2.4$. The nominal molar ratios for the silicalite sample are $\text{H}_2\text{O}:\text{Si}:\text{TPABr}:\text{Fe} = 3500:100:16.6:4.3$.

In each synthesis, the silicate source was added dropwise to the acidified iron or iron/aluminium source until a gel was

formed; 30 g of the gel was then transferred to a 50 ml, teflon-lined stainless steel autoclave; 2.54 g of TPABr was added to each autoclave along with 5 ml of a 1 M sodium metasilicate solution. The autoclave was then sealed and placed in a fan oven at 170°C for 72 h.

The resulting crystalline material was separated by filtration, and washed with deionized water. This will hereby be referred to as Na-Fe-ZSM-5(HT) (where HT refers to the catalyst being synthesized by hydrothermal methods). This was then calcined at 550°C in air for 4 h to remove the organic template. Following calcination, the sample was converted from Na-Fe-ZSM-5(HT) to H-Fe-ZSM-5(HT) by liquid phase ion-exchange over 16 h with a 1 M ammonium nitrate solution. This sample was then dried in vacuum at 100°C and activated by calcination at 900°C as described earlier to form Fe-ZSM-5(HT). Fe-ZSM-5(HT)(CVD) was synthesized from H-Fe-ZSM-5(HT) by CVD of FeCl_3 and calcined at 900°C as above. The silicalite sample was similarly calcined at 550°C in air for 4 h, treated with the 1 M ammonium nitrate solution and finally calcined at 900°C to produce Fe-Silicalite (HT).

2.2. Catalyst characterization

Specific surface areas and porosities were measured by nitrogen adsorption at 77 K using a Micrometrics ASAP 2010 apparatus. The samples were degassed at 200°C in vacuum for 12 h. The content of iron was determined by atomic absorption spectrometry. To verify the crystal structure of the synthesized zeolites, X-ray powder diffractograms were registered in the range $2\theta = 6\text{--}50^\circ$ using nickel filtered $\text{Cu K}\alpha$ radiation of the Phillips X'Pert X-ray diffractometer. Transmission electron microscopy was performed using Jeol JEM2010 Fastem operating at 200 keV. Samples were positioned on a carbon microgrid, supported on copper, by placing a few droplets of a suspension of ground sample in ethanol. The grid was then dried in ambient conditions.

2.3. Catalytic testing

Catalytic tests were carried out in a quartz tube (length 30 cm, i.d. 0.67 cm). The reactor was loaded with 0.5 g of the zeolite catalysts (pressed into tablets and crushed to 250–400 μm particle size), and pre-treatment was performed in situ at 400°C for 1 h in air to remove possible moisture and other contaminants from the zeolite. Toluene and other aromatic substrates were added by means of an evaporator equipped with a thermostat.

The reactions were usually performed at 350°C and atmospheric pressure. The ratio of aromatic substrate: N_2O :nitrogen (carrier gas) was 2:15:83 (mol%), with a total flow of 60 ml/min. Coke formation was excessive in hydrocarbon rich conditions. Analysis of the reactants and the products was carried out by on-line gas chromatography with FID detection (column: Rtx-5, 60 m \times 0.25 mm, o.d. = 0.4 mm,

d.f. = 1 μm). Following collection in a cooling trap, the products were further identified by GC/MS and by injection of reference materials. The mass balance during the sampling time was $\geq 95\%$. The selectivity (S) and yield (Y) were calculated according to $S_i = Y_i/X_{\text{aromatic}}$ and $Y_i = C_i/C_{\text{aromatic}}^0$, respectively, where X_{aromatic} is the conversion of aromatic substrate and C_{aromatic}^0 is the inlet concentration of aromatic substrate.

3. Results and discussion

Fig. 1 shows the evolution of products with time on stream resulting from toluene oxidation over $\text{N}_2\text{O}/\text{Fe-ZSM-5}$ catalysts prepared by different post-synthetic techniques. A number of polyaromatic structures were identified by GC/MS including naphthalene, methyl-naphthalene, anthracene, diphenylethane, which forms through the oxidizing dimerization of toluene, and large polycyclic structures such as benzantracene. Xylene isomers are also produced, along with small quantities of phenol and carbon oxides. The origin of benzene is not clear. It may arise from cracking of toluene or through a rapid oxidation of the benzylic CH_3 structure followed by decarboxylation.

It is evident from the results that Fe-zeolites prepared by CVD are far superior catalysts for the formation of mono-oxygenated products, and although these catalysts contain similar iron loading to the catalysts prepared by aqueous ion-exchange, it is clear that the nature of the active iron species in these samples differs significantly. An interesting result from this study is the absence of oxygenated products from attack by the active oxygen species at the methyl substituent.

Compared with conventional oxygen species that show a preference for the weaker C–H bonds of a substrate, the active oxygen species formed over $\text{N}_2\text{O}/\text{Fe-ZSM-5}$ (CVD) exhibits unusual electrophilic behaviour, where the stronger aromatic C–H bonds are preferentially targeted.

Table 2 presents product selectivities and some physico-chemical characteristics of the Fe-modified zeolites. Considering that a bond energy difference of ca. 70 kJ/mol exists between the aromatic C–H bonds and those of the methyl substituent, it is peculiar that the active oxygen species targets exclusively the stronger aromatic hydrogens. The methyl substituent is a weakly electron-donating group which, when attached to a benzene ring, renders it more susceptible to an electrophilic attack at the *ortho*- and *para*-positions. However, the catalytic oxidation of toluene over Fe-ZSM-5 (CVD), yields predominantly *para*-cresol, with the *ortho* and *meta* isomers being formed in comparable but smaller quantities. Such a result suggests that the methyl substituent imposes appreciable steric restrictions inside the zeolite micropore space, directing hydroxylation towards the more accessible *para*-position.

Fig. 2 summarizes the role of iron on the catalytic performance of Fe-zeolites prepared by chemical vapour deposition. Interestingly, with iron levels above 1 wt.% the yield to hydroxylated product diminishes significantly, possibly induced by the formation catalytically inactive iron oxide aggregates. Over the investigated range of iron loadings two areas of Fe-ZSM-5 catalytic activity are identified; below 1 wt.% iron, toluene conversion to cresols, benzene and polyaromatics increases steadily; above 1 wt.% iron, yields to cresols diminish, though the formation of benzene and polycyclic hydrocarbons continues.

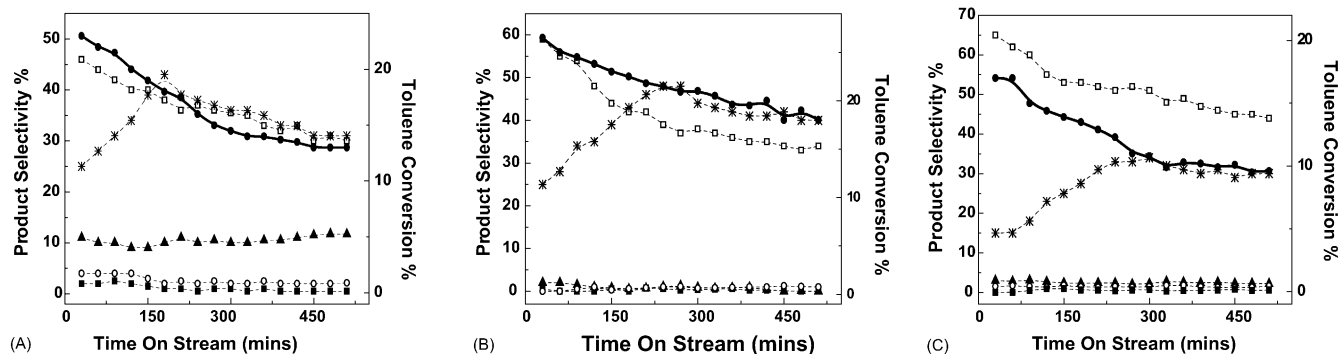


Fig. 1. Product evolution with time on stream for (A) 0.7% Fe-ZSM-5 (CVD), (B) 1.2% Fe-ZSM-5 (liquid phase ion-exchange) and (C) 0.35% Fe-ZSM-5 (solid state ion-exchange), 0.5 g catalyst, calcined at 900 °C, 15% N_2O , 2% toluene, balance N_2 , total flow 60 ml/min, temperature 350 °C, (●) toluene conversion, (□) benzene, (✱) polyaromatics, (▲) *p*-cresol, (○) *m*-cresol and (■) *o*-cresol.

Table 2

Product selectivities for Fe-ZSM-5 catalysts prepared by post-synthetic methods at ca. 20% toluene conversion

Preparation technique	Fe (wt.%)	A_{BET} (m^2/g)	V_{μ} (cm^3/g)	Cresols (%)	Benzene (%)	Polyaromatics (%)
Chemical vapour deposition (CVD)	0.7	425	0.168	19	40	34
Liquid phase ion-exchange	1.2	392	0.156	3	36	42
Solid state ion-exchange	0.35	441	0.171	4	63	21

Conditions: 0.5 g of Fe-ZSM-5, calcined at 900 °C, 15% N_2O , 2% toluene, balance N_2 , total flow 60 ml/min, reaction time 30 min.

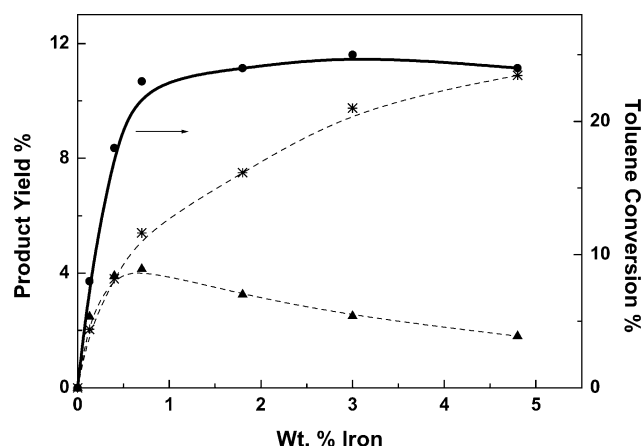


Fig. 2. Summary of (●) toluene conversion, (▲) total cresol yield and (✱) polyaromatic yield with increasing iron content for Fe-ZSM-5 zeolites (CVD), 0.5 g catalyst, calcined at 900 °C, 15% N₂O, 2% toluene, balance N₂, temperature 350 °C, total flow 60 ml/min, reaction time 30 min, W/F = 0.5 g s/ml.

The main problem during toluene oxidation is the rapid deactivation of the Fe-MFI catalyst due to coke formation. Fig. 3 shows that the deactivation process seems to depend essentially on the reaction conditions and chemical composition of the catalyst used. Under the indicated conditions and using 1.8 wt.% Fe-ZSM-5 (CVD) the catalyst micropore volume decreases severely, with a subsequent loss in catalytic activity. Increasing the iron loading also reduces the initial zeolite micropore volume, which could favour the accumulation of voluminous polyaromatic species within the micropore space.

The influence of the preparation procedure on the state of Fe-species in the different samples was visualized by means of representative TEM micrographs. Fig. 4(A) displays an electron micrograph taken under high-resolution conditions for the parent H-ZSM-5 sample, which was previously calcined at 900 °C. This sample clearly shows interference fringes (areas 1 and 2) of the ZSM-5 crystal structure with lattice d-spacing of ca. 2 nm. Fig. 4(C) shows 1.2% Fe-

ZSM-5 prepared by aqueous ion-exchange with the presence of an additional phase on its surface, which was not seen in the host H-ZSM-5 material (Fig. 4(B)). It has been shown that the formation of Fe(III) ion species, especially the FeOOH-hydroxides in solution, result in the creation of aggregated oxide clusters, which are not active for the decomposition of nitrogen oxides [45–47]. Fig. 4(D) displays a TEM micrograph of 0.4% Fe-ZSM-5 prepared by the vapour-phase deposition of FeCl₃ into the ZSM-5 matrix. Comparison of this image with those obtained previously by aqueous ion exchange suggests that the iron species is highly dispersed inside the zeolite channels, with no significant agglomeration on the external catalyst surface.

X-ray diffractograms of the synthesised Fe-ZSM-5 catalysts and their silicalite analogues exhibited high crystallinity in all cases (Fig. 5). Table 3 summarizes the catalytic performance of Fe-ZSM-5 catalysts prepared by CVD and hydrothermal methods. Iron species encapsulated in the ZSM-5 matrix lose their ability to activate molecular oxygen, evidenced by the low yield to mono-oxygenated products when air is employed as oxidant. Aerial oxidation of toluene affects the substrate skeleton with benzene being liberated to the product stream. Similarly, many attempts to accomplish the one-step direct oxidation of benzene with molecular oxygen proved unsuccessful due to the destruction of the aromatic ring and low phenol yields [48]. Nitrous oxide is a much milder oxidant but forms a highly electrophilic oxygen species upon decomposition, which is capable of inserting itself into the stronger aromatic C–H bonds. Reactions using mechanical mixtures of Fe₂O₃/H-ZSM-5 demonstrate that the superior cresol formation of the N₂O/Fe-ZSM-5 (CVD) catalyst cannot be explained by the simple dispersal of iron oxide in these samples.

Table 3 also presents catalytic data for the oxidation of toluene over Fe-ZSM-5 catalysts prepared by hydrothermal synthesis (HT). No activity was observed for Na-Fe-ZSM-5 catalysts, which contained iron embedded in lattice positions. H-Fe-ZSM-5 catalysts, which also contain iron in framework positions, displayed better activities though

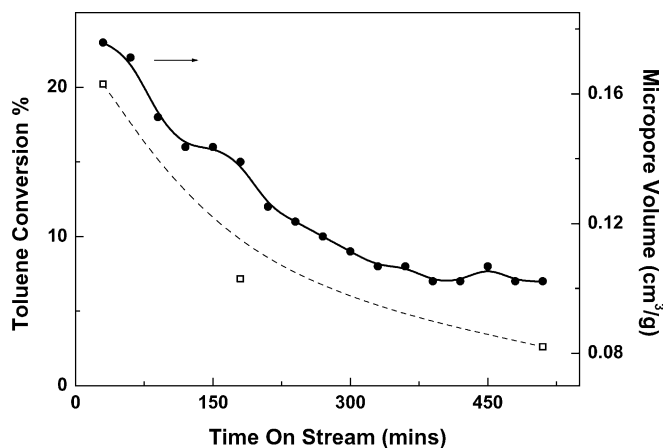


Fig. 3. Influence of reaction conditions on (●) toluene conversion and (□) zeolite micropore volume, 0.5 g of 1.8% Fe-ZSM-5 (CVD), calcined at 900 °C, 15% N₂O, 2% toluene, balance N₂, total flow 25 ml/min, temperature 350 °C.

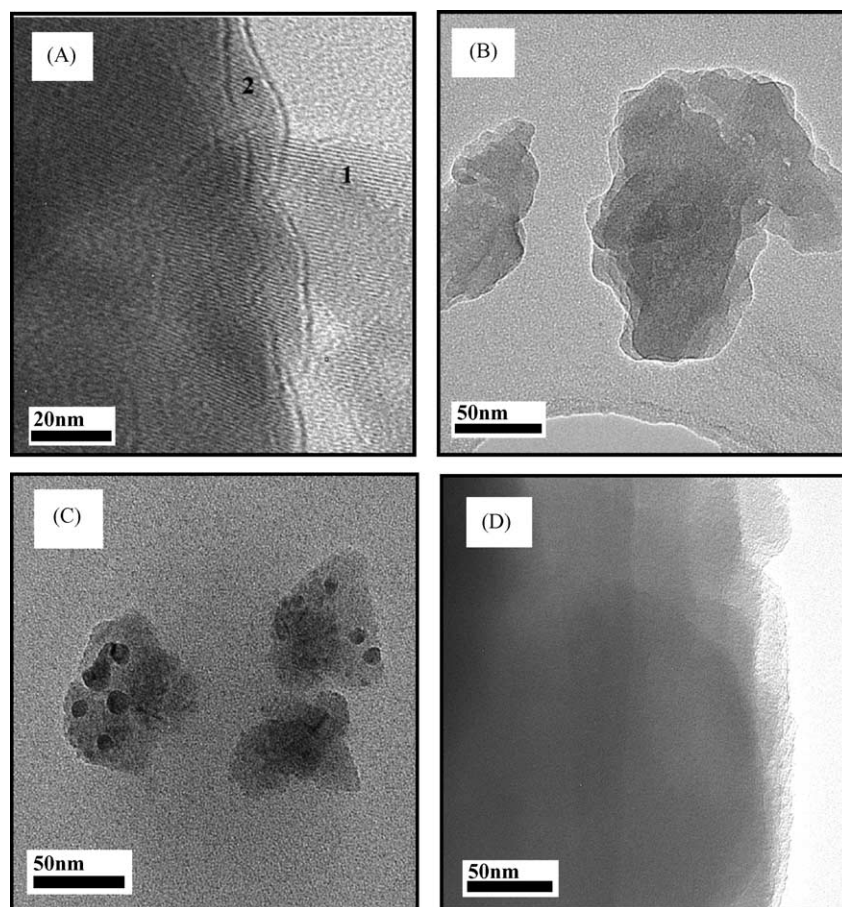


Fig. 4. Transmission electron micrographs of ZSM-5 particles after activation at 900 °C: (A) high resolution TEM of ZSM-5 crystal structure; (B) medium resolution TEM of H-ZSM-5 particle morphology before iron incorporation; (C) TEM micrographs of 1.2% Fe-ZSM-5 prepared by liquid phase ion-exchange; (D) TEM micrograph of 0.4% Fe-ZSM-5 prepared by chemical vapour deposition.

the yield to hydroxylated product was low. Following high-temperature treatment to provoke migration of iron into extraframework positions forming Fe-ZSM-5, a significant

increase in cresol yields was observed. The results lend credence to the model that Fe sites in extralattice positions are crucial for these hydroxylation reactions. Addition of

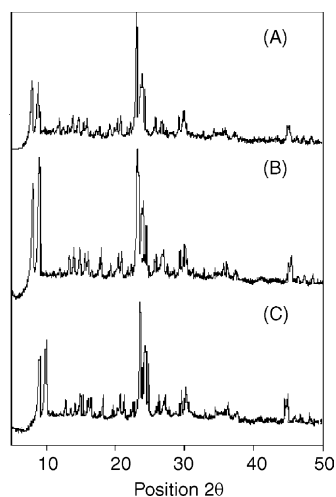


Fig. 5. X-ray diffractograms of (A) 1.3% Fe-Silicalite, (B) 0.4% Fe-ZSM-5 and (C) H-ZSM-5 prepared by hydrothermal synthesis.

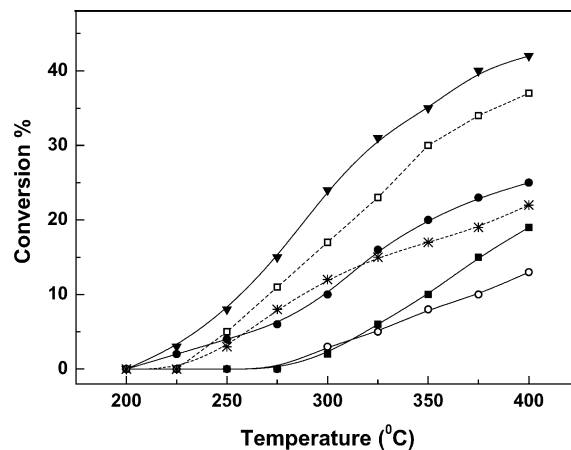
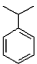
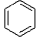
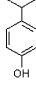
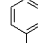
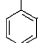
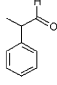
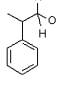
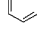
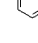
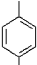
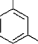
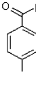
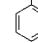
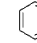
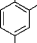
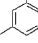
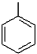

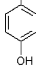
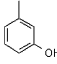
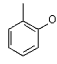
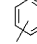
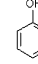
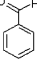
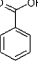
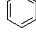
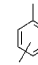
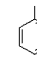
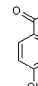
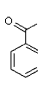
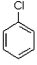
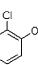
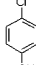
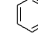
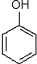
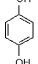
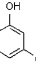
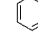


Fig. 6. Reactivity of (▼) isopropylbenzene, (□) *para*-xylene, (●) toluene, (*) benzaldehyde, (■) chlorobenzene and (○) phenol over 0.5 g of 0.4% Fe-ZSM-5 (CVD), calcined at 900 °C, 15% N₂O, 2% substrate, balance N₂, temperature 350 °C, total flow 60 ml/min, reaction time 30 min, W/F = 0.5 g s/ml.

Table 4
Summary of product distributions at 350 °C for 0.5 g of 0.4% Fe-ZSM-5 prepared by CVD

Substrate	X%	Product Selectivity (%)					Minor Products			
Isopropylbenzene		36	20	19	13					
	35									Poly-Aromatics
<i>para</i>-Xylene		77	6							
	30									
Toluene		48	15	22						
	20			Poly-Aromatics						
Benzaldehyde		54	38							
	17							Poly-Aromatics		
Chlorobenzene		62	12							
	11						Poly-Aromatics			
Phenol		82	13							
	7									

Conditions: 0.5 g of 0.4% Fe-ZSM-5 (CVD), calcined at 900 °C, 15% N₂O, 2% substrate, balance N₂, total flow 60 ml/min, reaction time 30 min, W/F = 0.5 gs/ml.

catalyst produces mainly *ortho*-chlorophenol and smaller quantities of *para*-chlorophenol. The chlorine substituent is weakly deactivating and promotes oxidative attack at the *ortho*- and *para*-positions of the aromatic ring.

4. Conclusion

The decomposition of nitrous oxide over iron species in extra-framework positions of MFI zeolite produces a highly electrophilic oxygen species capable of introducing hydroxy function into a variety of aromatics substrates. Such iron species can be created by chemical vapour deposition of anhydrous FeCl₃ or by high-temperature treatment of hydrothermally synthesized zeolites, though higher alcohol yields have been achieved with the latter. The oxidation of aromatics possessing bulky alkyl groups over N₂O/Fe-ZSM-5 is strongly influenced by steric restrictions within the micropore space, limiting the yield of hydroxylated product and favouring secondary reactions affecting the side groups. For the oxidation of smaller aromatic substrates, the active oxygen species is influenced by the activating/deactivating nature of the substituent groups.

Acknowledgements

The authors would like to thank Enterprise Ireland for financial support and Miroslav Mihov for TEM analysis.

References

- [1] A. Belansky, J. Haber, Oxygen in Catalysis, Marcel Dekker, New York, 1996.
- [2] G.K. Borekov, Catalytic activation of dioxygen, in: J. Andersen, M. Boudart (Eds.), Catalysis: Science and Technology, Springer, Berlin, 1982, p. 40.
- [3] M.A. Pepera, J.L. Callahan, M.J. Desmond, E.C. Milberger, P.R. Blum, N.J. Bremer, J. Am. Chem. Soc. 107 (1985) 4883.
- [4] L.A. Bradzil, A.M. Ebner, J.F. Bradzil, J. Catal. 163 (1996) 117.
- [5] C.R. Adams, T.J. Jennings, J. Catal. 2 (1963) 63.
- [6] C.R. Adams, T.J. Jennings, J. Catal. 3 (1964) 549.
- [7] V.D. Sokolovskii, Catal. Rev. Sci. Eng. 32 (1990) 1.
- [8] J. Lee, J.J. Grobowski, Chem. Rev. 92 (1992) 1611.
- [9] J.R. Monnier, In: Proceedings of the Third World Conference on Oxidation Catalysis, Amsterdam, 1997, p. 135.
- [10] C. Batiot, B.K. Hodnett, Appl. Catal. A 137 (1996) 179.
- [11] G.I. Panov, A.S. Kharitonov, V.I. Sobolev, Appl. Catal. A 98 (1993) 1.
- [12] G.I. Panov, V.I. Sobolev, K.A. Dubkov, V.N. Parmon, N.S. Ovanesyan, A.E. Shilov, A.A. Shteinman, React. Kinet. Catal. Lett. 61 (1997) 251.

- [13] G.I. Panov, A.K. Uriarte, M.A. Rodkin, V.I. Sobolev, *Catal. Today* 41 (1998) 365.
- [14] US Patent 5,110,995 (1992).
- [15] V.L. Zholobenko, L.M. Kustov, V.B. Kazansky, In: *Proceedings of the Ninth International Conference on Zeolites*, vol. 2, Butterworth, Montreal, 1992, p. 299.
- [16] E. Suzuki, K. Nakashiro, Y. Ono, *Chem. Lett.* 6 (1988) 953.
- [17] G.I. Panov, V.I. Sobolev, A.S. Kharitonov, *J. Mol. Catal.* 61 (1990) 85.
- [18] J. Zhu, S.C. Tsang, *Catal. Today* 81 (2003) 673.
- [19] J. Miki, Y. Osada, T. Konoshi, Y. Tachibana, T. Shikada, *Appl. Catal. A* 137 (1996) 93.
- [20] S.L.H. Rebelo, M.M.Q. Simoes, M.G.P.M.S. Neves, J.A.S. Cavaleiro, *J. Mol. Catal. A* 201 (2003) 9.
- [21] M. Hassan Zahedi-Niaki, S.M. Javaid Zaidi, S. Kaliaguine, *Appl. Catal. A* 196 (2000) 9.
- [22] S. Velu, N. Shah, T.M. Jyothi, S. Sivasanker, *Micropor. Mesopor. Mater.* 33 (1999) 61.
- [23] A.P. Singh, T. Selvam, *J. Mol. Catal. A* 113 (1996) 489.
- [24] A. Tuel, Y. Ben Taarit, *Appl. Catal. A* 102 (1993) 201.
- [25] M.P. Vinod, T.K. Das, A.J. Chandwadkar, K. Vijayamohanan, J.G. Chandwadkar, *Mater. Chem. Phys.* 58 (1999) 37.
- [26] D.A. Bulushev, L. Kiwi-Minsker, V.I. Zaikovskii, O.B. Lapina, A.A. Ivanov, S.I. Reshetnikov, A. Renken, *Appl. Catal. A* 202 (2000) 243.
- [27] V. Parvulescu, C. Constantin, B.L. Su, *J. Mol. Catal. A* 202 (2003) 171.
- [28] R. Burch, C. Howitt, *Appl. Catal. A* 103 (1993) 135.
- [29] P. Kubanek, B. Wichterlova, Z. Sobalik, *J. Catal.* 211 (2002) 109.
- [30] P. Marturano, L. Drozdova, A. Kogelbauer, R. Prins, *J. Catal.* 192 (2000) 236.
- [31] G. Berlier, G. Spoto, S. Bordiga, G. Ricchiardi, P. Fiscaro, A. Zecchina, I. Rossetti, E. Selli, L. Forni, E. Giamello, C. Lamberti, *J. Catal.* 208 (2002) 64.
- [32] A.M. Ferretti, C. Oliva, L. Forni, G. Berlier, A. Zecchina, C. Lamberti, *J. Catal.* 208 (2002) 83.
- [33] J. Perez-Ramirez, F. Kapteijn, J.C. Groen, A. Domenech, G. Mul, J.A. Moulijn, *J. Catal.* 214 (2003) 83.
- [34] V.I. Sobolev, K.A. Dubkov, E.A. Paukshtis, L.V. Pirutko, M.A. Rodkin, A.S. Kharitonov, G.I. Panov, *Appl. Catal. A* 141 (1996) 185.
- [35] J. Jia, K.S. Pillai, W.M.H. Sachtler, *J. Catal.* 221 (2004) 119.
- [36] H.-Y. Chen, W.M.H. Sachtler, *Catal. Today* 42 (1998) 73.
- [37] H.-Y. Chen, T. Voskoboinikov, W.M.H. Sachtler, *J. Catal.* 180 (1998) 171.
- [38] E.-M. El-Malki, R.A. van Santen, W.M.H. Sachtler, *J. Catal.* 196 (2000) 212.
- [39] K. Yamada, C. Pophal, K. Segawa, *Micropor. Mesopor. Mater.* 21 (1998) 549.
- [40] Heinrich, C. Schmidt, E. Löffler, W. Grunert, *Catal. Commun.* 2 (2001) 317.
- [41] M. Rauscher, K. Kesore, R. Monnig, W. Schwieger, A. Tissler, T. Turek, *Appl. Catal. A* 184 (1999) 249.
- [42] A.A. Battiston, J.H. Bitter, F.M.F. de Groot, A.R. Overweg, O. Stephan, J.A. van Bokhoven, P.J. Kooyman, C. van der Spek, G. Vanko, D.C. Koningsberger, *J. Catal.* 213 (2003) 251.
- [43] H.-Y. Chen, E.-M. El-Malki, X. Wang, R.A. van Santen, W.M.H. Sachtler, *J. Mol. Catal. A* 162 (2000) 159.
- [44] M. Kogel, R. Monnig, W. Schwieger, A. Tissler, T. Turek, *J. Catal.* 182 (1999) 470.
- [45] Y. Li, J.N. Armor, *Appl. Catal. B* 2 (1993) 239.
- [46] S. Sato, Y. Yu-u, H. Yahiro, N. Mizuno, M. Iwamoto, *Appl. Catal.* 70 (1991) 1.
- [47] B. Coq, D. Tachon, F. Figueras, G. Mabilon, M. Prigent, *Appl. Catal. B* 6 (1995) 271.
- [48] I. Yamanaka, M. Katagiri, S. Takenaka, K. Otsuka, *Stud. Surf. Sci. Catal. A* 130 (2000) 809.
- [49] A. Ribera, I.W.C.E. Arends, S. de Vries, J. Perez-Ramirez, R.A. Sheldon, *J. Catal.* 195 (2000) 287.